Removal of Tritiated Methane from Gaseous Xenon for use in Dark Matter Detectors

Clint Richardson

May 6, 2011

Abstract

Dark Matter detection relies on very precise, well calibrated, and ever growing detectors. Liquid Xenon detectors represent a strong candidate for dark matter detection because of xenon's good qualities as a detector medium. LUX, a Liquid Xenon detector, which is worked on by the Experimental Nuclear Research group here at the University of Maryland, is a good example of such a detector. Its large mass, capable shielding, and low background levels put it at the forefront of dark matter detection. Currently, LUX uses external sources of radiation for calibration. However, the non-uniformity of external sources, compounded by the self-shielding of the detector, make them undesirable for use in calibration of such large detectors. A much more efficient, and ideal, way is to use an internal source. Use of such a source though, risks permanent contamination of the detector. Presented is work done demonstrating the ability to remove Tritiated Methane (CH3T) from gaseous xenon, in order to show it a viable option for use in internal calibration.

Introduction

1 DARK MATTER

Experimental evidence suggests the existence of massive particles that interact only via the gravitational and weak forces [1]. These hypothetical particles are collectively termed Dark Matter. One potential candidate particle is the Weakly Interacting Massive Particle (WIMP). The rotational speed of galaxies in particular suggests that some new type of matter exists. Observed rotational speeds flatten out at higher radii from the galactic center, but if only the luminous matter were present, they would reach a peak and then fall off ($v \propto M/r$) [1]. This flattening out of speeds can be explained by a density of matter which is both greater than the density of luminous matter, and uniform so that the ratio $M/r \approx const.$ In order to account for the effect of this matter on the rotational speeds of galactic arms, theoretical models suggest that a Dark Matter halo

exists around our galaxy and that this halo flows through our galaxy as a type of wind. This wind would then also flow through the earth. While the majority of Dark Matter particles will flow through the earth without interacting with anything, if they are WIMPs, a very small fraction may recoil off of atomic nuclei. A detector with a sufficiently calibrated energy scale, background rejection factor, and large enough target mass, may see a handful of events a year. Such a discovery would revolutionize our current understanding of matter and the universe.

1.1 The WIMP Miracle

Whatever the Dark Matter consists of, during the early stages of the Universe, when the temperature of the Universe was greater than the mass of the Dark Matter particles, the DM particles were created by, and interacted with, the rest of the primordial soup frequently. However, as soon as the temperature of the universe cooled below the DM mass scale, it became much less likely that DM particles would have been created by a two particle collision. After this epoch, the DM particles, while still annihilating with one another, were not being created anymore. Hence, their number was dropping. Annihilation only took place when a DM particle and its anti-particle could meet, so as the Universe continued to expand and the DM particles rarefied with it, it became much less likely that they could annihilate. After a certain rarity was reached, they essentially ceased to annihilate. This cessation, in conjunction with the fact that they were no longer being created, means that the number of DM particles became fixed. The final number of DM particles varies as their annihilation cross section. In order to account for current DM density, that cross section must have been on the order of $10^{-9}\ GeV^{-2}$[2]. However, experimental results show that a typical cross section for particles interacting only via the weak force is on the same order of magnitude [2]. Therefore, the cross section needed to explain current DM density is also on the order of weak scale interactions! This fortuitous result is the WIMP miracle, and is also a driving force of the inspiration behind the exploration for WIMPS.

1.2 Detection of WIMPs

1.2.1 Indirect Detection via Neutrinos

One possible manner of indirectly detecting WIMPS lies in neutrino detection. WIMPS that become gravitationally trapped inside the Earth or Sun should build up over time, increasing WIMP density in the region and thus the odds of WIMP annihilation. Such annihilation would produce highly energetic neutrinos that could be detected. Such neutrinos would be easily differentiated from cosmic or solar backgrounds because of their much greater energy. Detection of these highly energetic neutrinos would constitute a strong suggestion of the existence of WIMPS.

1.2.2 Direct Detection

WIMPS, by definition, have a probability of scattering off of nucleii through weak interactions. Hence, any detector capable of seeing the recoiling nucleii from such scatterings, could theoretically detect WIMPS by this means. However, the low probability of WIMP scattering means that such detectors must have very low background rates and large target mass in order to have any hope of directly detecting WIMP-caused nuclear recoil. Further, because the WIMP momentum has a range of possible values, the energy of a recoil event also has a distribution of possible of values. Therefore, the detector must have a very low background rate over the whole energy range of interest (several KeV!). Detection of such a signal however, would consitute the most concrete and exciting evidence for the existence of WIMPS.

2 XENON DETECTORS

2.1 BENEFITS OF XENON IN DIRECT DETECTION

Xenon serves as a good detector medium for a variety of reasons. First, it has no long lived radioactive isotopes. Second, it has a high atomic number (Z=54), and in liquid form has a high density (~3g/cm^3), which combine to give a Liquid Xenon detector a high stopping power. This stopping power preserves the center of the detector from background radiation, and thereby enhances the efficacy of fiducial cuts. Cross sections for WIMP interactions vary as the square of the atomic mass number, which means that xenon ($A \approx 132$) has a relatively large cross section for detecting WIMPs. Further, it has a relatively high boiling point (for noble gases), which means less of a demand on cooling systems for Liquid Xenon detectors.

2.2 SIGNALS IN A XENON DETECTOR

The two most important types of events that occur in a dual phase (liquid/gas) xenon detector are nuclear recoil and electron recoil. Gamma rays or beta particles can recoil off of the electrons of the xenon atoms, causing emission of a new beta particle and a photon. That is to say, in electron recoil, xenon gives off scintillation light and charged particles [3]. The energy of the reaction distributes itself between these two products in an anti-correlated manner. The scintillation light can be measured using Photo-Multiplier Tubes. The emitted electrons can be drifted via a strong electric field to an anode located above the surface of the liquid. As they accelerate toward the anode, they will pick up enough energy to excite other electrons in the xenon gas. These excited electrons will then fall back to their ground state and give off a second source of scintillation light. The energy of the original scintillation (defined as S1) can be compared to the energy of the light given off by the excited electrons (defined as S2). The magnitude of S2 will be directly related to the initial energy of the electron emitted in the recoil event. Hence, comparing the ratio of

S1 to S2 of many events will give the average distribution of energy in electron recoil events. Nuclear recoil events also produce scintillation light and charged particles. However, the average ratio of energy distribution between S1 and S2 is different than the average for electron recoil. Hence, in order to know what type of event is happening in your detector, you need to know very precisely the distribution and the average of the ratio S1/S2 for both electron and nuclear recoil events. Further, you need to know these two things in your detector. The efficiency of your detector varies over its volume and so it is not possible to to use measurements of the difference between nuclear recoil events and electron recoil events taken elsewhere to calibrate your detector. Both types of events must be well understood in order for quality data analysis to occur. Knowing just one or the other will allow for fiducial cuts to maximize the number of events of a certain type, but we need to discriminate between the two. Therefore, we need to know to what confidence level we can say that signals are not caused by electron recoil while also knowing what percentage of nuclear recoil events we must throw out because of overlap of the two spectra.

2.3 LUX

LUX is a dual phase time projection chamber (TPC) xenon detector searching for possible nuclear recoil events due to WIMP scattering off of atomic nucleii. It consists of an internal chamber where 350 kg of xenon serve as the target mass [4]. This chamber is then shielded by a 300 ton water tank; the tank is futher equipped with photo-multiplier tubes (PMTs) that allow for cosmic ray veto via Cerenko radiation detection. The detector itself has two banks of photo-multiplier tubes. One, in the bottom of the vessel, submerged beneath the Liquid Xenon, collects initial scintillation light (S1) from recoil events. The charge of the event is drifted via an electric field through the liquid until it reaches the gas phase, where upon acceleration, it produces another scintillation signal (S2) via excitation of orbital electrons. The charge itself is collected on a grid of wires, and the electronic signal is then dismissed. The second bank of PMTs however, above the surface of the Liquid Xenon, collects the S2 signal. Location of the S2 signal gives the x and y coordinates of the recoil event, while the time difference between S1 and S2 allows for knowledge of the z coordinate. The location of the event, as well as the ratio of S1/S2 allows for a strong ability to discriminate between nuclear and electron recoil, if the detector is properly calibrated.

2.4 CALIBRATION OF A DETECTOR

2.4.1 Energy Scale calibration

In order to know the energy of events in a detector one must obviously know the energy scale of the detector. A simple way to learn this is to use radioactive sources with known energies to generate events in the detector and use this information to calibrate your energy scale. Common sources include Fe-55 and

Ba-133. However, these sources, while emitting well-known energies, produce mono-energetic spectra. The peaks of these spectra will more precisely determine the energy scale of the detector, but they will only give the ratio of S1/S2 for one specific energy. While a source that emits a spectrum does not calibrate the energy scale as precisely as a mono-energetic peak, it works well enough in practice, and further has the important benefit of giving S1/S2 for the entire energy range of interest.

2.4.2 Event Discrimination Calibration

In order to know that a detected signal comes from dark matter, one must know what type of event created it. As stated above, one can discriminate between nuclear and electron recoil by making fiducial cuts in the data based on the average ratio of S1/S2. In order to make these cuts, the detector's reaction to nuclear and electron recoil events must be well understood. Beta and gamma emitters are often used to calibrate the detector's reaction to electron recoil events, while neutron sources are used to calibrate its reaction to nuclear recoil events. Both types of events must be well characterized to make precise and correct data cuts.

2.4.3 Tritium as a Beta Source

Tritium has several beneficial qualities as a beta-source for electron recoil events. First, it emits beta particles in a continuum with a Q-value of 18 keV. The continuum of energies allows for a more precise calibration of S1/S2 across the energy range of interest. Tritium's continuum also conveniently covers the energy range of interest in WIMP detection in Liquid Xenon. Second, it emits only a single beta particle, which further helps in the determination of S1/S2. However, tritium, being an isotope of hydrogen, has large diffusion and permeability constants. These could allow for tritium to diffuse into the surfaces of the detector. The tritium would then slowly diffuse back into the detector throughout the course of any experiment, adding to the background rate. Further, bare tritium is highly chemically active and could easily stick to the walls of the detector. These problems are compounded by tritium's relatively long half-life ($\sim$12 years). With this half-life, simply waiting for the tritium to decay away is not feasible.

2.4.4 Tritiated Methane as a Beta Source

Tritiated methane (CH3T) solves many of the problems inherent in using bare tritium. Its larger size means a smaller diffusion constant. Also, it is a chemically inert gas, and therefore ought not stick to the surfaces of the detector.

R & D at The University of Maryland

Limitations on This and Future Generations

Current external calibration techniques are less than ideal for LUX, and will be even worse for planned, larger, next generation detectors. The self-shielding of these detectors, coupled with the non-uniformity of the external source radiation, will inhibit accurate calibration of S1/S2 throughout the detector volume. The clearest remedy to these difficulties is to use an internal calibration source. Internal sources, especially if dissolved throughout the detector medium, will give very accurate measurements of detector performance throughout the detector volume. As stated earlier, for the calibration to be as successful as possible, the source radiation must span the energy range of interest. Hence, any dissolved source not removed from the detector after calibration will necessarily contribute to background levels in the energy range of interest, and, if not removed to a sufficient level, could potentially ruin the detector. Therefore, before detector calibration can be pursued using internally dissolved sources, the ability to remove these sources after calibration must be shown. The Experimental Nuclear Reseach Group at The University of Maryland has been experimenting with the ability of removing an internally dissolved calibration source (CH3T) from gaseous xenon. Such work represents a first step toward removal from Liquid Xenon, and so also a first step toward calibration of the next generation of dark matter detectors, as well as an important procedure for the best performance of LUX.

3 Detector Setup

Our setup design (Figure 1) consists of a plumbing system and the detector electronics. The plumbing system has three main parts: a xenon system, a methane system and a transfer system. The detector itself consists of a proportional tube with a maintained voltage of 2 kV between the inner wire and the outer surface when in use. Gases are moved around the plumbing by the use of liquid nitrogen (LN). Immersing any part of the plumbing in LN will cause the xenon at that location to begin to freeze. As it freezes, it causes a pressure drop, which brings more of the xenon in the system to that location, which then in turn freezes and so on. We call this technique cryopumping.

3.1 Plumbing System

3.1.1 METHANE SYSTEM

The purpose of the methane system is, essentially, storage. It consists of two (2) one gallon stainless steel storage bottles and a methane purifier. The storage

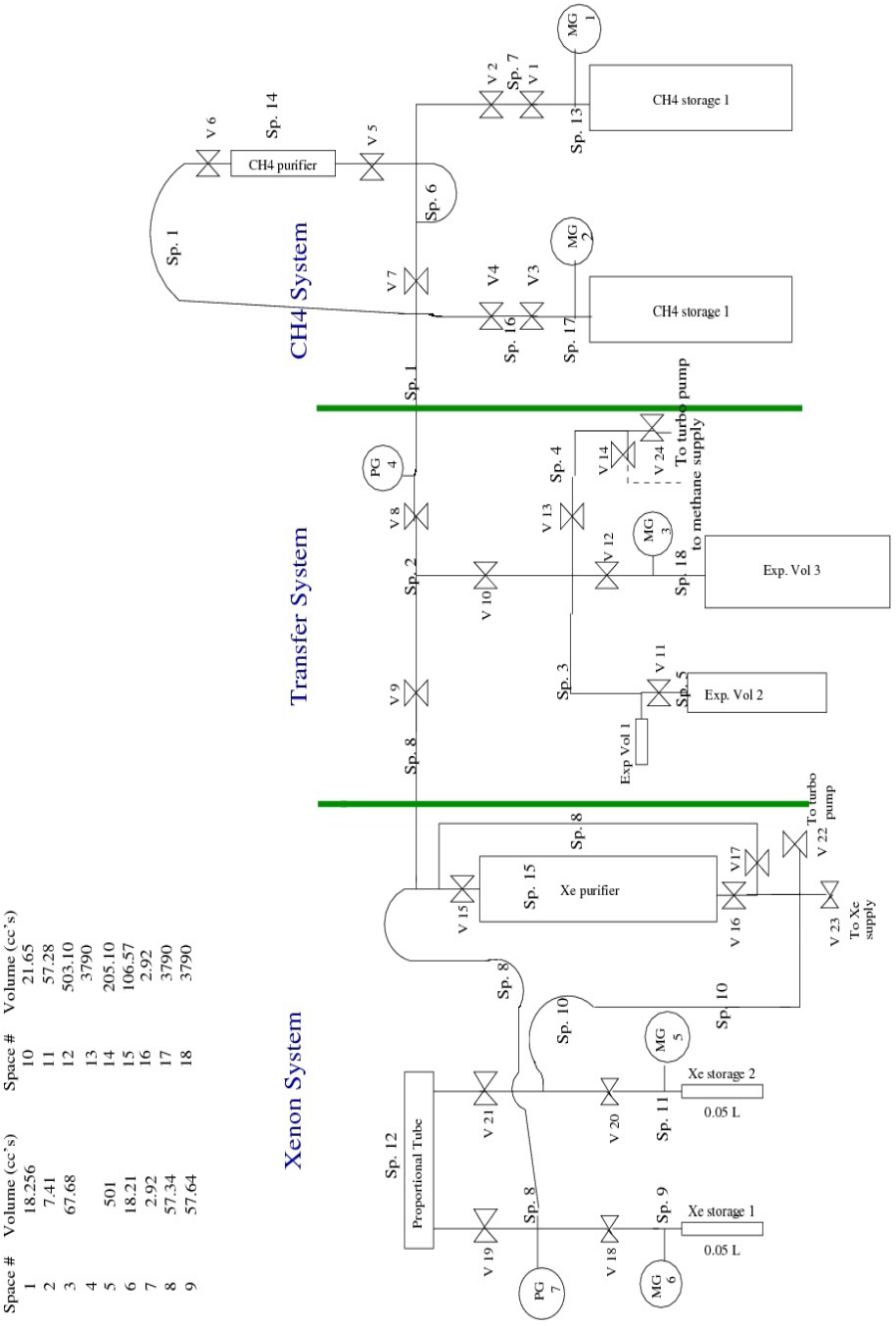

Space #	Volume (cc's)	Space #	Volume (cc's)
1	18.256	10	21.65
2	7.41	11	57.28
3	67.68	12	503.10
4		13	3790
5	501	14	205.10
6	18.21	15	106.57
7	2.92	16	2.92
8	57.34	17	3790
9	57.64	18	3790

Figure 1: Experimental Setup with volumes listed. The volume of Space 4 was not calculated because it was never used. Hourglasses correspond to Valves. MG and PG stand for Mechanical Gauge and Piezo Gauge respectively.

bottles are used to contain a gaseous combination of tritiated methane and regular methane. The total intitial amount of methane stored was 855 mg (the total amount of methane injected throughout the course of the experiment is less than 2 mg), with a total intial activity of 5 mCi. The methane purifier was installed to take out any impurities potentially left over from manufacturing. The methane purifier was never used but remains on the system. Stored methane in the methane system can be injected into the xenon gas through the transfer system.

3.1.2 TRANSFER SYSTEM

Too large of an injection of methane would saturate the purifier and swamp the electronics. Further, imprecisions or inconsistencies in injection amounts would introduce new variables into the data. Hence, it is necessary to have an ability to control the amount of methane injected. We accomplish this by use of the transfer system. The transfer system consists of a transfer volume (Space 2), valved off from both the methane system and the xenon system, and connected to a series of expansion volumes. Opening Valves 3, 4 and 8 expose the transfer volume to the methane in storage bottle 2. The amount in this transfer volume can be regulated via cryopumping (any excess can be put back into storage bottle 2 and closed off once the pressure on PG 1 reaches the desired level). However, for small injections, PG 1 is not accurate enough to calculate the amount of methane in the transfer volume. If the amount is known at a higher pressure though, opening up Space 2 to the different expansion volumes allows for a rarefaction to desired levels with precision. Once Space 2 has the desired amount of methane, it can be closed off from these expansion volumes. The methane can then be injected into the xenon system.

3.1.3 XENON SYSTEM

The xenon system houses the proportional tube as well as the xenon purifier (SAES # PS3-MT3-R-1), which uses a hot zirconium getter to purify. Once methane has been injected, its activity can be detected in the proportional tube. The xenon/methane mixture can then be flowed through the purifier in order to remove the methane. The xenon system consists of two storage bottles, a proportional tube, a xenon purifier, and a purifier bypass. All of the parts of the system are connected by 1/4 inch stainless steel pipe and are separated either by hand valves (Swagelok part #6-LV-DFHFR4-P-GR) or all-metal high pressure valves (Swagelok part #:SS-4UW-V51). The same is true for the rest of the plumbing systems. Pressures are known via digital Piezo Gauges (MKS series 902) as well as mechanical pressure gauges (PGU-40-PC30-C-4FSF). The Piezo Gauges are used for precision measurements, while the mechanical gauges serve mostly to inform one of when gas is being stored in a bottle.

The proportional tube dominates the volume of the Xenon System ($\sim$75%) and hence also contains the vast majority of both xenon, and any injected CH3T. This minimizes the amount of CH3T outside of the proportional tube.

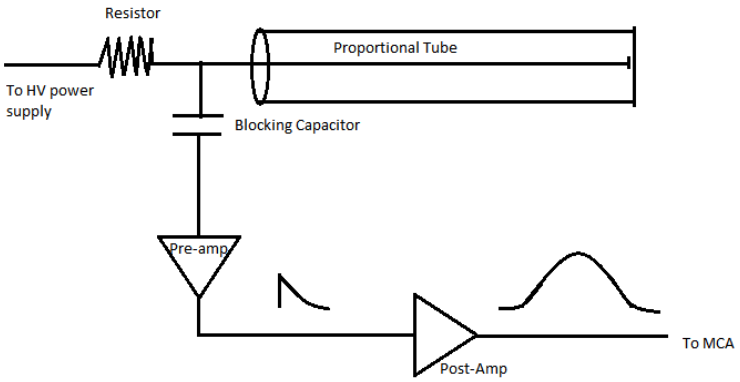

Figure 2: Detector Electronics: A High-Voltage power supply maintains a constant voltage between the inside and outside of the proportional tube, while a strong resistor ensures no loss of signal to ground and a blocking capacitor keeps the preamp at a low voltage. The signal from the preamp is then shaped into a gaussian and sent to the MCA.

3.2 Detector Electronics

As the tritium beta decays in the detector, the emitted electrons are drifted toward the wire at the center of the proportional tube by a constant voltage mainted by a high voltage power supply (See Figure 2). When the electrons get close enough to the wire, they move very quickly, ionizing other atoms and causing an electron cascade. This cascade (as well as the effects due to the positive ions being repelled by the strong electric field) is read out as a current pulse. The current pulse is transmitted to a preamp (Amptek A250), which is kept at low voltage by means of a blocking capacitor. The emitted signal of the preamp is then shaped to become more of a gaussian, which in turn is read by our Multi-Channel Analyzer (MCA). The height of the initial current pulse, and therefore also of the signal which reaches the MCA, is proportional to the energy of the primary event. The MCA bins these pulses in terms of their height and transmits them to a software program that turns them into a histogram. The MCA has 1024 Channels (bins) and a 5 volt input range.

4 Procedures

4.1 Injections

When injecting, Valves 3 and 4 are opened to expose space 1 to the methane. Once equilibrium is reached, immersion of methane storage bottle 2 in LN allows for cryopumping of the methane back into the storage bottle. Valves 3 and 4 are then closed when the desired pressure has been reached on PG4. The transfer volume (space 2) is exposed to the methane and then isolated from the methane system. Once the injection itself is prepared, the xenon gas in the xenon system is cryopumped into xenon storage 1. When this stage of cryopumping is reached and PG7 reads $\sim$0.1 torr, Valve 9 is opened to allow the methane to expand into the xenon system. After waiting several minutes for the system to reach equilibrium, Valve 9 is closed to isolate the transfer system from the xenon system. Valve 18 is also closed to confine the xenon/methane mixture in xenon storage bottle 1. The xenon methane mixture is then warmed up while still in storage bottle 1. Once warm, Valve 18 is opened to allow the mixture to populate the xenon system. Once equilibrium has been reached, the detector is allowed to run for several minutes in order to take a spectrum of the injection. This completes the injection.

4.2 Purifications

After the injection run has been completed it is necessary to purify the gas in order to determine our ability to remove the methane from the xenon. The purification process starts by cryopumping all of the xenon/methane mixture into xenon storage bottle 1. Once the system reaches xenon vapor pressure, Valve 18 is closed and the mixture is allowed to warm up. At this point, Valves 17 and 21 are closed to prohibit the gas from bypassing the purifier. Then, the lower purifier isolation Valve (Valve 16) is opened, while keeping Valve 15 closed, and xenon storage bottle 2 is immersed in LN. Next, the xenon/methane mixture is allowed to populate spaces 8,9,12 (everything upstream of the purifier). When the system reaches equilibrium, pressure and time measurements are made in order to determine flow rate. Valve 15 is then opened and regulated by hand for the duration of the purification. Once the pressure on PG7 reaches $\sim$150 torr, Valve 15 is closed and purification stops. The remaining gas upstream of the purifier is then cryopumped back into xenon storage bottle 1, while the remaining gas downstream of the purifier continues to collect in xenon storage bottle 2; Valves 18 and 20 are then closed to isolate both pockets of gas. Valve 16 is closed to isolate the purifier. Next, the xenon that has passed through the purifier is allowed to fill the system by opening Valves 17,20,21. A detector run is then started using the Fe-55 to confirm that the detector still works. Once confirmed, an overnight run is started in order to see how much, if any CH3T has been left in the detector. This is the end of purification.

4.3 Re-purification

Initial results showed a lack of 100% purification. Hence, it was desirable to purify twice between injections, thereby hopefully returning the system to its state before the injection occured. This allows for an essentially fresh start for each injection. In order to re-purify, xenon storage bottle 1 is immersed in LN. Once it reaches LN temp, Valve 18 is opened and the entirety of the gas goes to xenon storage bottle 1. Valves 17 and 21 are then closed again to isolate the purifier, but now both Valves 15 and 16 are opened. Xenon storage bottle 2 is immersed in LN and once the xenon in storage bottle 1 has warmed, purification occurs by cracking open Valve 18. This valve is then hand regulated for the duration of re-purification. Once the entirety of the gas has been purified, the purifier is isolated and the clean gas is allowed to populate the system (a small part being cryopumped back to storage bottle 1 in order to return the system to its initial pressure setting). At this point, another Fe-55 run takes place, and then a background run occurs over night.

Data Analysis

5 Calibration of the Detector

Iron-55 was used as a calibration source. It emits x-rays with energy 5.9 keV. Figure 3 shows an overnight run with an Fe-55 source externally placed next to the detector. The peak occurs at Channel 406 and has a FWHM of 70 Channels. This gives an energy resolution of $\pm 17\%$ with a total energy range of interest of 4.2 - 14.5 keV and bin size of 0.015 keV. This range is well within the energy range of tritium decay. A tritium spectrum is shown in Figure 4.

6 Previous Results of Removing Methane from Gaseous Xenon

Previously, the Experimental Nuclear Research Group has studied the removal of regular methane (CH4) from gaseous xenon. A similar purifier was used (SAES # PS4-MT3-R-1). The data showed that purifier performance depended on temperature, flow rate, and purifier rest time [5]. Figure 5 shows the results. The data was gathered via mass spectroscopy, using a Residual Gas Analyzer (RGA). While these data give evidence of the ability of the purifier to remove CH4, two reasons compelled further investigation. First, CH3T could always potentially have significantly different chemical properties then CH4, and the ability to remove CH4 does not guarantee the ability to remove CH3T. Second, because the data was taken using mass spectroscopy, all the data tells us is the purity of the xenon gas at the RGA. It does not address surface contamination throughout the detector. Measuring this type of contamination via CH3T is

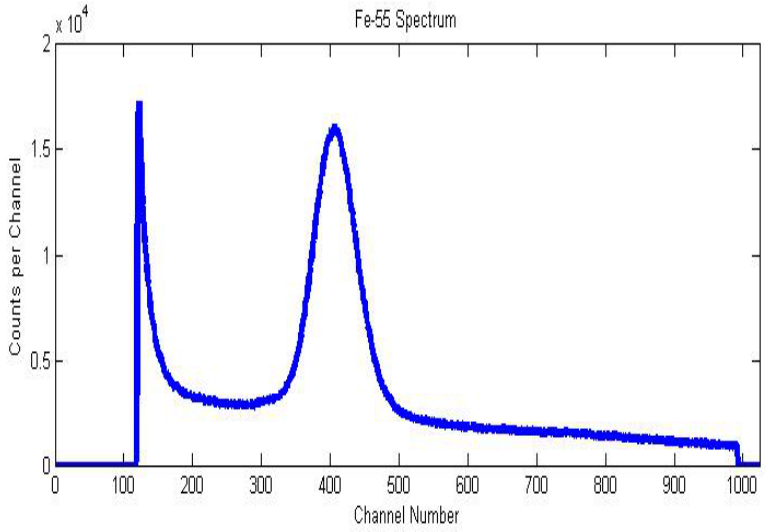

Figure 3: Fe-55 Spectrum with 5.9 keV energy peak at Channel 406. Apparent peak to the left is from electronic noise and is not a true signal. From the peak, we infer an energy scale of 69 Channels per keV. Run time was approximately one week.

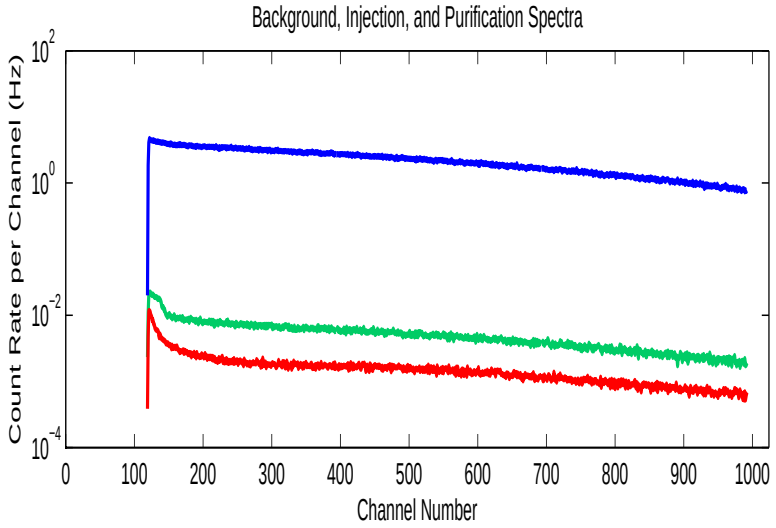

Figure 4: Tritium Spectrum (Blue) compared to Background Spectrum (Red) and a spectrum after one purification (Green). Spectra were taken using vastly different run times ($\sim$10 min for the Tritium viz. $\sim$1 day for the Background/Purification). Energy range over Channels 100-1000 is 1.4 - 14.9 keV.

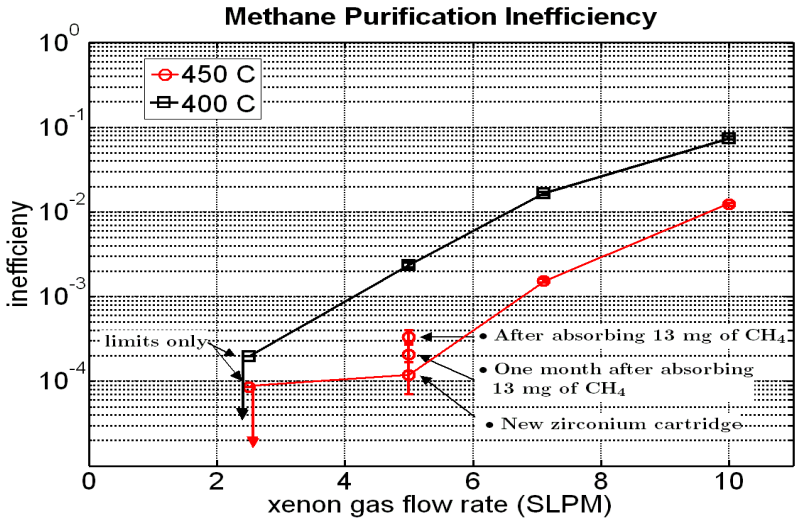

Figure 5: Previous Results of the Removal of CH4 from gaseous xenon. Purity is measured via mass spectroscopy using a Residual Gas Analyzer (RGA) [5].

relatively straight forward using our setup. These considerations prompted the building of our setup to test the ability of removing CH3T from xenon.

7 One Pass Purification Data

Data was collected by integrating count rates over 703 channels (channels 288-991). This range was chosen to minimize the contribution of electronic noise to the data. Uncertainties in integrated (total) count rates follow a Poisson distribution, where $\sigma_{Rate} = \sqrt{N}/T$, with N =Number of Counts and T =Total Run Time. One pass purification rate was calculated by the following formula:

$$P_{\%} = 100 * [1 - (C_p - B)/(C_I - B)]$$

$C_p =$ Total Count Rate after one purification

$C_I =$ Total Count Rate after injection

$B =$ Total Background Count Rate prior to injection

Typical data runs after one purification were one day in length, while typical injection runs lasted minutes. After the first purification, the gas was re-purified and data from the run after this purification was used as the background rate prior to injection for the next injection. These runs also typically lasted a day.

Initial results showed purifier performance of less than 100%. In order to ascertain the causes of this less than 100% purification rate, two variables were

Table 1: Fraction of CH3T activity removed in one pass. Rest days are defined as number of days between injections.

Run #	Avg. Flow Rate (SLPM)	Rest Days	One Pass Purification %
46	0.113 ± 0.004	30	99.8415 ± 0.0005
49	0.111 ± 0.004	5	99.461 ± 0.001
53	0.27 ± 0.01	10	99.8463 ± 0.0004
56	0.47 ± 0.02	5	99.581 ± 0.007
59	0.238 ± 0.009	5	99.6818 ± 0.0006
62	0.123 ± 0.005	2	98.755 ± 0.003
67	0.33 ± 0.01	2	99.874 ± 0.004
72	0.135 ± 0.005	5	99.5000 ± 0.0009
77	0.201 ± 0.008	2	99.299 ± 0.001
83	0.48 ± 0.02	3	99.536 ± 0.001
89	0.240 ± 0.009	2	98.590 ± 0.002
95	0.233 ± 0.009	2	99.533 ± 0.001
100	0.42 ± 0.02	11	99.045 ± 0.002
105	0.44 ± 0.02	3	99.416 ± 0.002

investigated: flow rate through the purifier and days between injections. If the gas flows too quickly, it could pass through the purifier without bonding to the zirconium. Hence, a faster flow rate through the purifier increases the chance that the methane will penetrate through it and remain in the system. Therefore, flow rate was selected as a variable of interest. Only the surface of the zirconium in the purifier actually removes impurities, and as this surface gets filled up over the course of many purifications, the purifier loses its ability to work correctly. However, as time passes, the impurities on the surface will diffuse into the bulk of the zirconium, freeing up space on the surface to purify again. The magnitude of this effect was not known prior to our experiments and hence, the number of days between injections (rest days) was chosen as a variable of interest. Days between injections is a preferable variable to days between purifications because, while one pass purification rates were less than 100%, the amount of methane left over in the system is trivial compared to that injected. Therefore, the dominating effect in taking up space on the surface of the zirconium comes from injections.

Three flow rates were selected: 0.1, 0.2, and 0.4 SLPM. While real life imprecisions dictated an impossibility of obtaining those exact values, and uncertainty exists in instaneous flow rate, the average flow rate over the total purification often fell very close to these values. Average flow rate was measured by timing the total time that the gas flowed through the purifier and taking note of the pressure at PG7 before and after purification in order to know the quantity of gas purified. Three rest times were selected: 2-3, 5, and 10+ days. These were constrained by time (it takes a month to get 3 data points for the longest rest time) and the intial conception that the purifier should recover its capabilities

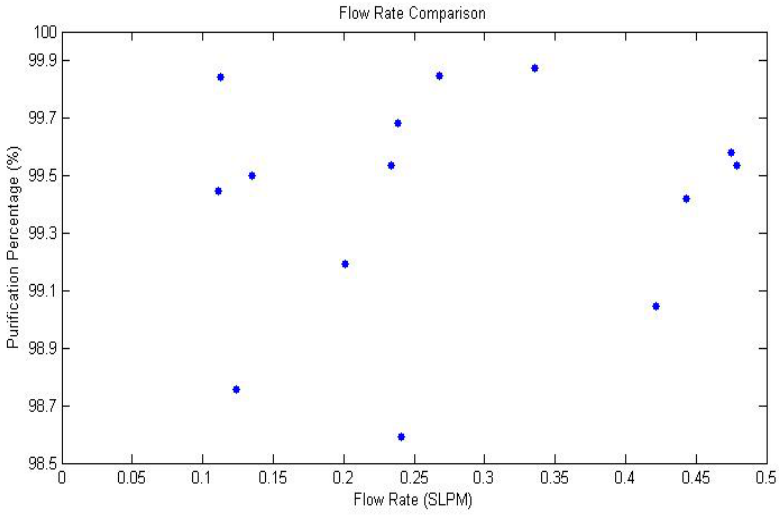

Figure 6: One-Pass Purifier Performance is plotted for each run versus that run's average flow rate during purification.

within a matter of days. Fourteen data points were collected, with data being taken at least once for each flow rate at each amount of rest time. Some data points were then taken again to test the repeatability of the result. Table 1 shows the results for all 14 data points. Figures 6, 7 show plots of one pass purification rate versus flow rate and rest time respectively. As one can see, no clear relationship shows itself between purifier perfomance and flow rate. Figure 7 suggests some dependence of purifier performance on rest time, but it is clearly not well established (Note: statistical uncertainty error bars lie within the points themselves and hence have not been shown in the figures).

In order to go farther with the data, average purification percentages were taken of each flow rate for a given rest time, and also each rest time for a given flow rate. This averaging yields three data points for each graph (the flow rates and rest times were binned according to the afore selected desired values). While the statistical uncertainties yield negligible error bars, the standard deviation of the averages must be taken into account. Hence, plotted on these graphs are error bars corresponding to one standard deviation of each average. Figure 8 shows a potentially siginficant difference between average purifier performance at 2-3 days rest time and at 5 days rest time. No claims can be made about rest time of 10 days because of its large error bars. However, this average also has the fewest number of data points (3). That fact, in addition to it having the highest average purification rate, and the significant difference between 2-3 and 5 rest days suggest that the purifier performance is dependent upon rest time, which is in agreement with our hypothesis. Further, calculating a χ^2 value comparing the individual points to their average yields a p-value of 0.12 which

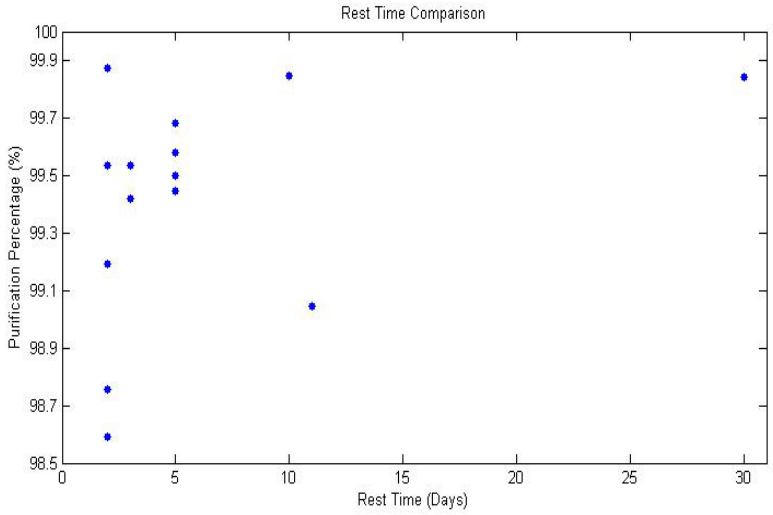

Figure 7: One-Pass Purification Performance is plotted versus the number of rest days for the purifier. A single rest day is defined as one day since the last injection. Because initial purifications always take place on the same day as the injection, ten rest days signifies that ten days have passed since the purifier last saw a large amount of CH3T.

is suggestive of a significant dependence.

Figure 9 shows a remarkable similarity of average purifier performance versus flow rate. None of these data points differ significantly from one another. Hence, the data suggest that purifier performance does not depend on flow rate in our setup. Calculating a χ^2value for this distribution yields a p-value of 0.96, which further confirms that there is no reliance in the data on flow rate.

8 Background Data after Two Purifications

8.1 Initial Results

After each one pass purification run was completed, the gas was re-purified and a new run started. Over the course of the experiment, the total background count rate over Channels 288-991 increased. This increase, while not monotonic, did rise overall as a function of number of injections. The total count rate of the initial run of the semester (Run44) was subtracted from the total count rate of each successive background run in order to demonstrate an increase in background levels. Figure 10 shows this increase (error bars are not plotted because they lie within the points themselves), and Table 2 contains the data from each run. Further, when one looks at the spectra of the difference between the runs, the difference takes a shape typical of Tritium. Figure 11 shows this

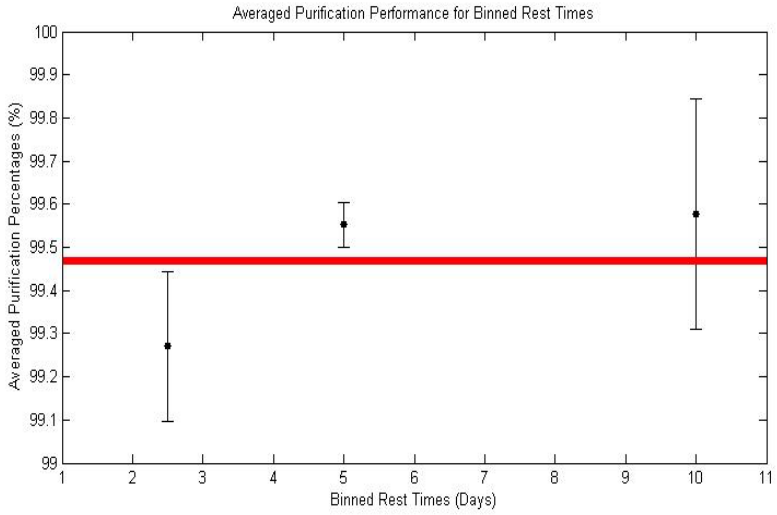

Figure 8: Averaged Purification Rate for Each Binned Rest Time. Data points are plotted in blue with their average (99.47%) plotted as a red line.

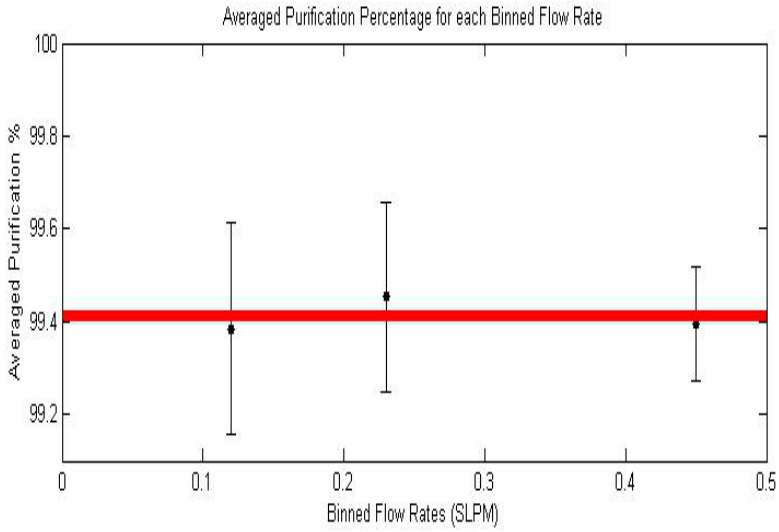

Figure 9: Average Purification Rate for Each Flow Rate. Data points are plotted in blue with their average (99.41%) plotted as an orange line.

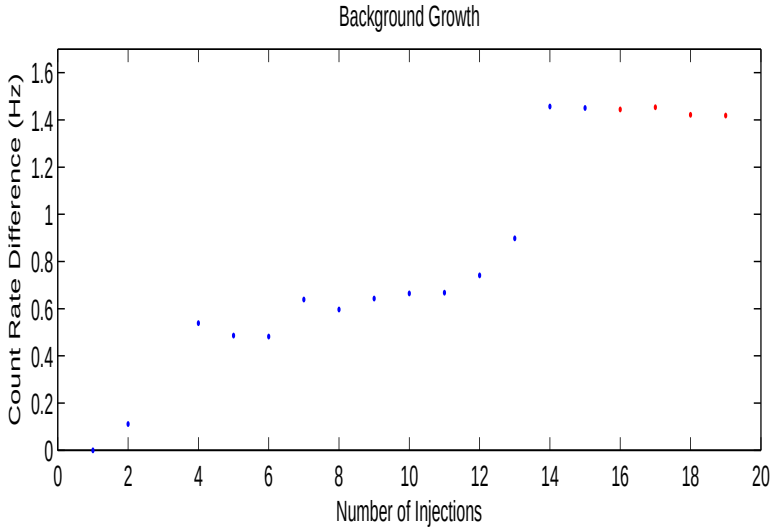

Figure 10: After re-purification runs, the background rate is compared to that of Run 44 in order to discern any long term changes in background levels. Blue data points correspond to re-purification runs following an injection, while red data points do not actually have injections between them and are simply successive purifications.

result by comparing Run 44 with Run 102.

8.2 Subsequent Re-purifications

When first pass purification data taking was complete, the gas in the system was re-purified an additional four times in an effort to return to initial background levels. As with previous data, Run 44 was subtracted from these new spectra and the count rates were summed over Channels 288-991. The resulting total count rates from these purifications are also plotted on Figure 10 and correspond to points 16-19 on the x-axis (Note: No new injections were completed after injection 15, thus every point before what is labeled injection 16 was taken in the same manner - injection, purification, re-purification, background run - while every point including and after what is labeled injection 16 was taken in the following sequence: additional purification, background run). As evidenced, additional purifications have not returned the background rate in the detector to original levels. Further, with the cessation of injections, the background levels in the detector have ceased to rise. Based on this result, it is plausible that CH3T remains somewhere in the system. Either it has diffused into the parts of the detector, or it is sticking to the walls.

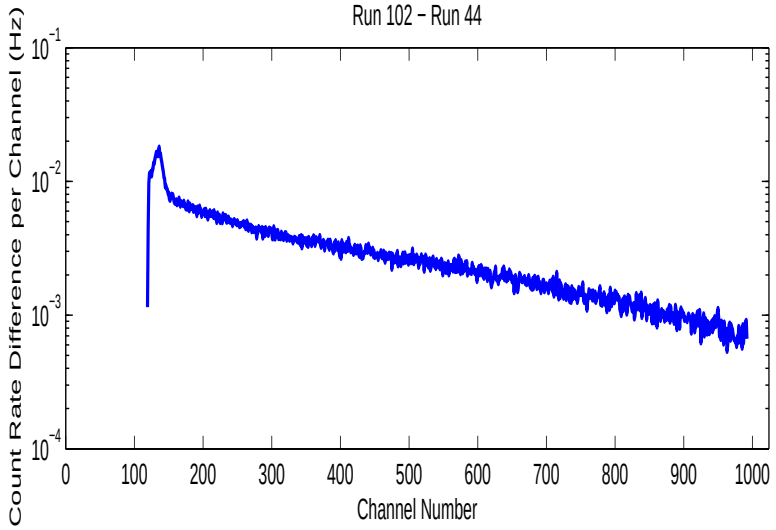

Figure 11: Count Rate Difference per Channel between Run 102 and Run 44. The shape of the resulting spectrum follows the expected form of tritium spectra.

Table 2: Background Results after Re-purification.

Run #	Count Rate (Hz)	Change from Run 44 (Hz)	# of Injections
44	0.887± 0.002	0	1
47	0.997± 0.002	0.111±0.003	2
54	1.426± 0.004	0.539±0.005	4
57	1.373± 0.004	0.486±0.005	5
60	1.369± 0.004	0.482±0.005	6
64	1.525± 0.004	0.639±0.005	7
69	1.483± 0.005	0.596±0.005	8
74	1.530± 0.005	0.643±0.005	9
80	1.552± 0.005	0.665±0.005	10
86	1.555± 0.005	0.668±0.005	11
91	1.628± 0.004	0.741±0.005	12
97	1.784± 0.005	0.898±0.005	13
102	2.344± 0.004	1.457±0.004	14
107	2.337± 0.006	1.451±0.006	15
109	2.331± 0.006	1.444±0.006	15
111	2.341± 0.005	1.454±0.006	15
113	2.309± 0.006	1.422±0.006	15
115	2.306± 0.002	1.419±0.003	15

8.3 Potential Causes

The background rate in the detector has been shown to have grown as a function of number of injections. Further, it has been shown that additional purifications beyond two yield little effect on this background rate. Hence, it is likely that either tritium or CH3T remains somewhere in the parts of the detector. Perhaps when CH3T passes near the high voltage wire, the tritium frees itself from the methane and, having the characteristics described above, either sticks to chemically, or diffuses into, detector parts. Alternatively, the high voltage wire itself could have absorbed some tritium or CH3T. Further, imprecisions in cryopumping could potentially account for some of the excess. One can never get below xenon vapor pressure when cryopumping, and at this pressure CH3T will not freeze at LN temperatures. Therefore, one cannot know for sure that the CH3T has followed the xenon through the plumbing. In order to test the effects of this, the system will be hooked up to a turbo pump and evacuated over the course of a few days. Any remaining CH3T after such evacuation must be either in the xenon or somewhere in the detector parts. Depending on the outcome of this test, the entire system may be wrapped in heater tape in order to bake out any CH3T or tritium remaining in the detector parts, or the high voltage wire in the proportional tube may be swapped out for a new, clean one. These tests and those mentioned regarding flow rate will be undertaken this summer.

Looking closer at Figure 10, two data points clearly stick out: the point after 4 injections and the point after 14 (corresponding to Runs 54 and 102 respectively). These data points show the largest increases among the data and mark two quasi-tiers of background growth. In order to understand what could have caused these jumps, several variables were investigated: DAQ functionality, first pass flow rate, rest time, amount of time the CH3T spent in the detector before being purified, and how long it could have potentially spent in the detector at xenon vapor pressure. During the both Runs 54 and 102 the DAQ had acquisition problems. Our MCA software is not the most reliable, and in both cases needed to be restarted during the background run. However, this has happened during several other runs and not yielded such significant leaps and so it is not likely to be the cause. Perhaps the initial purification flow rate could somehow affect the results. It turned out that initial purification had occurred at all three flow rates, (two injections occurred between Run 47 and Run 54 yielding three total injections in need of investigation). Hence, it is doubtful that this has was the cause of such marked growth. Further, the three data cycles of interest were collected at two of the three rest times, 5 and 10 days, yet none of the other data points at these rest times showed such a dramatic increase. During the injections prior to each data point, the unpurified gas spent an average of 51 minutes in the proportional tube, while the average for the whole set was greater than 54 minutes, and so it is not likely that amount of time in the detector caused these dramatic increases. Lastly, because we allow the CH3T to fill the detector at xenon vapor pressure, perhaps the longer it spends in the detector at this low pressure, the more likely it is to stick to or diffuse into the detector parts. However, while the average of this time for Runs 54 and 102

was above the average for all runs (10.67 min compared to 9.3 min), there were several runs that had similar times and they did not all yield significant growth. Taking all of this together, it is not clear why such jumps in background rate occurred at these data points. However, they were not the only points which showed statistically significant growth, and it seems that the background rate growth depends on number of injections more than any other variable.

9 Systematic Errors

9.1 In Flow Rate

The lack of dependence on flow rate in our data may arise from imprecisions in purification procedure. Valve 15 (the valve used to regulate flow rate during initial purification) admits of difficulty in precision, especially at the beginning of the purification. The large pressure differential during the initial stage of purification makes regulation of the flow rate challenging. The first 10% of the gas through the purifier most likely has a much higher flow rate than the average. Because the average flow rates are so modest, the pocket of gas that rushes through the purifier (and hence presumably has a significantly higher impurity concentration) has the potential to dominate the background after purification. Since approximately the first 10% of the gas has the same difficulty of controlling, regardless of intended flow rate, it is probable that a similar amount quickly penetrates the purifier every time. This phenomenon would explain the near identical averages of purification efficiency for each flow rate, as well as the clear lack of dependence of our data on flow rate. In order to test this theory, an electronic read-out will be connected to PG7 that will be capable of giving instantaneous pressure drop (and thus flow rate) throughout purification. Such data will show the amount of variance between the initial flow rate and the average. If it is significantly higher, a new high pressure valve will be installed above the purifier and data sets will be repeated to see if better control of the initial flow rate yields a difference in the data.

Conclusion

One-Pass Purification rates of methane from xenon exceeding 99% can regularly be achieved at a variety of flow rates and rest times. Purifier rest time seems to affect the purification efficiency. However, at least for our small flow rates, the data suggest that flow rate does not affect purifier performance in our setup. The background rate in the detector has been shown to have grown as a function of number of injections. Further, it has been shown that additional purifications beyond 2 yield little effect on this background. This is evidence of a small level of permanent contamination. Several simple experiments can be done to further the investigation into removal of CH3T from gaseous xenon. Namely, an electronic read-out connected to PG7, coupled with a new all-metal

high pressure valve installed in place of the current Valve 15, will give more precise control and better monitoring of flow rate. These improvements, because of the possibility that a transient flow rate is dominating the background after purification, will more clearly show whether or not flow rate affects purifier performance in our detector. Further, because it is possible that CH3T doesn't freeze into the xenon ice, but instead remains behind in the detector, pumping by means of a turbo-pump on the ice will remove any such remnants, and demonstrate whether or not imprecisions in cryopumping account for discrepancies and growths in background rates. Additionally, swapping out the current high voltage wire for a new one will show whether or not contamination is localized to the wire, while baking the detector will demonstrate whether or not surface contamination is accounting for this increase. Lastly, if none of the above tests allow for a return to original background levels, simply installing a new purifier cartridge will perhaps allow for such a return.

In the end, while more is needed to be done to know fully about the ability to remove CH3T from xenon in our system, the regularity of one-pass purification rates exceeding 99% efficiency indicates that this is a promising avenue of investigation. The work conducted shows the viability of using CH3T as an internal calibration source, and will hopefully inspire the investigation of its removal from Liquid Xenon in order to ensure the ideal functioning of LUX.

Acknowledgments

I would like to thank Dr. Carter Hall for his invaluable advice, knowledge and mentoring throughout the course of my work with the Experimental Nuclear Research Group. Further, I would like to thank Wes Szamotula for his help in conducting the experiments as well as Attila Dobi, Simon Slutsky, and the rest of the Experimental Nuclear Research Group for their help and advice throughout.

References

[1] D'Amico, Guido et al. . arXiv:0907.1912 [astro-ph.CO]

[2] Griest, K. et al. Phys.Rept. 333 (2000) 167-182

[3] Aprile, E. et al. Rev.Mod.Phys. 82 (2010) 2053-2097

[4] Fiorucci, S. et al. AIP Conf.Proc. 1200 (2010) 977-980

[5] Dobi, A. et al. Nucl.Instrum.Meth. A620 (2010) 594-598